Atomic and electronic structure of quasiperiodic and crystalline Mg-61 at.% Al alloys

1999 J. Phys.: Condens. Matter 11 191

(http://iopscience.iop.org/0953-8984/11/1/016)

J. Phys.: Condens. Matter **11** (1999) 191–208. Printed in the UK PII: S0953-8984(99)95590-X

Atomic and electronic structure of quasiperiodic and crystalline Mg–61 at.% Al alloys

Vincent Fournée†, Esther Belin-Ferré†*, Anne Sadoc‡§, Patricia Donnadieu‖, Anne Marie Flank§ and Herbert Müller¶

† LCPMR UMR 7614 and GDR CINQ, 11 rue Pierre et Marie Curie, F-75231 Paris Cédex 05, France

‡ LPMS and GDR CINQ, Université de Cergy-Pontoise, 5 Mail Gay-Lussac, Neuville sur Oise, F-95031 Cergy-Pontoise Cédex, France

§ LURE, CNRS, MENESR, CEA, Bâtiment 209D, Centre Universitaire Paris-Sud, BP 34, F-91898 Orsay Cédex, France

‖ LTPCM-ENSEG, GPM and GDR CINQ, BP 75, Domaine Universitaire, F-38402 Saint Martin d'Hères, France

¶ Institut für Experimentalphysik, Technique Universitat, 6-8 Wiedner Haupstrasse, A-1080 Vienna, Austria

Received 6 July 1998, in final form 4 September 1998

Abstract. Mg–Al alloys with composition Mg–61 at.% Al display two types of structure: a stable crystalline state (the so-called β-Mg_2Al_3) and a metastable one showing both quasiperiodicity and inflation symmetry. The atomic as well as electronic structures of stable crystalline β-Mg_2Al_3 and a metastable $Mg_{39}Al_{61}$ phase that exhibits quasiperiodicity and inflation symmetry have been studied thanks to x-ray spectroscopy techniques. Extended x-ray absorption fine-structure experiments performed above the Al and Mg K absorption edges have probed the local atomic order around Mg as well as Al atoms. X-ray emission and absorption spectroscopies have investigated occupied and unoccupied electronic states around Mg and Al. The local order has been found to be the same around Al atoms in both alloys, whereas around Mg atoms differences are seen for higher shells than first neighbours. This suggests that the same clusters must be involved in both phases and that the quasiperiodicity is connected with modification of the Mg atom environment forming the linkage between large clusters. On the other hand, the electronic distributions show differences from β-Mg_2Al_3 to the quasiperiodic phase that are consistent with the local order studies. A pseudogap is observed in the Mg and Al electronic structures which is more marked in the quasiperiodic phase than the crystalline alloy. By analogy to quasicrystals, we suggest the enhancement observed is due to the occurrence of an inflation mechanism in the arrangement of the clusters in the quasiperiodic alloy with respect to the β-Mg_2Al_3 crystal.

1. Introduction

In the Mg–Al Franck–Kasper system, Donnadieu *et al* (1996) have recognized that according to elaboration conditions, for the nominal composition Mg–61 at.% Al, a metastable quasiperiodic phase (QP) forms which transforms upon annealing into a stable crystalline phase having a structure usually referred to as the β-Mg_2Al_3 one. The crystalline alloy possesses a large

* Contact author: Esther Belin-Ferré, LCPMR, URA CNRS 7614 and GDR CINQ, 11 rue P et M Curie, 75231 Paris Cédex 05, France. E-mail address: belin@ccr.jussieu.fr.

0953-8984/99/010191+18$19.50

cubic cell which is decorated with a complex packing of tetrahedral and icosahedral clusters (Samson 1965). Therefore, the metastable QP state structure is connected to the cubic point group. In addition, it displays an inflation symmetry characterized by the ratio $2 + \sqrt{3}$. From the crystallographic point of view, this QP phase can be indexed as an incommensurate three-dimensional modulation of a three-dimensional mean lattice (Yamamoto 1982). Within that framework, the inflation symmetry is a consequence of a particular value of the modulation wave vector. This QP phase may thus be considered as a cubic quasicrystal. Hence, in order to investigate possible correlation between quasiperiodicity and the atomic and electronic structures of crystalline counterparts, it is of interest to use this Mg–61 at.% Al system. In addition, in contrast to many other approximant/quasicrystal systems, the Mg–Al one contains no transition metal. It is also worth mentioning that up to now, comparison between approximants and quasicrystals has often been limited by the fact that they displayed differences in nominal compositions.

We have undertaken EXAFS measurements of the QP phase and β-Mg_2Al_3 alloy as such a study brings insight into the local atomic arrangement (Sadoc *et al* 1993). Our aim was not only to compare local order in the QP phase and β-Mg_2Al_3 alloy but also to investigate whether the local order of the latter alloy is consistent with the Samson model. This basic information is necessary to build the atomic structure of the QP phase, which is still unknown in detail, and will be, in any case, very hard to solve from direct methods. Preliminary results have been reported so far elsewhere (Sadoc *et al* 1998). On the other hand, atomic and electronic structures being closely connected, it might be relevant to carry out an investigation of the electronic structures of the QP and β-phases comparatively. For such a purpose, x-ray emission and photoabsorption spectroscopies (labelled XES and XAS hereafter respectively) are very useful techniques. Indeed, they probe separately partial occupied and unoccupied electronic distributions around each kind of atom of a solid (Agarwal 1979, Bonnelle 1987). First results have already been obtained on both QP and β-Mg_2Al_3 alloys (Fournée *et al* 1998, Belin-Ferré *et al* 1998).

In this paper we present data that involves the preliminary results that have been complemented by new measurements. It is organized in several sections. The second one refers to the experimental methodologies. Section 3 describes the results which are discussed in section 4 and a conclusion is given in the last section.

2. Experiment

2.1. Samples

The samples were prepared at the Centre d'Etudes de Chimie Métallurgique–Centre National de la Recherche Scientifique of Vitry (France). Mg and Al metals of purity >99.99% were used. A first ingot was produced by melting appropriate amounts of Mg and Al in a graphite crucible kept in an argon atmosphere. Then, it was melted repeated times by means of high frequency induction in order to obtain a homogeneous phase. Rapid solidification using the planar flow casting method allowed us to obtain quenched ribbons of the QP phase with composition Mg–61% Al atoms. Further annealing at 600 K made it possible to produce the stable crystalline β-Mg_2Al_3 alloy (Donnadieu *et al* 1996).

2.2. X-ray spectroscopy techniques

X-ray spectroscopy techniques are very useful as they allow us to gain insight into the electronic and atomic structures of a material. Indeed, XES and XAS techniques probe separately

s, p, d, ... occupied and unoccupied states, respectively, around each component of a solid. The transitions obey dipole selection rules: $\Delta l = \pm 1$, $\Delta j = 0, \pm 1$. Whereas p states are obtained alone, s and d states are probed all together; however, transitions to d states, when possible, are favoured with respect to transitions to s states. The transition probabilities are constant or vary slowly against energy. Consequently, direct information is obtained on the probed partial local densities of states (DOSs) within energy ranges as large as a few tens of eV but no absolute values of DOS are reached. For a given element in various samples, changes in the shapes of the spectral energy distribution curves can be directly connected to changes in the probed partial densities of states. When the XAS spectra are recorded over wider energy ranges, namely a few hundreds of eV, it is no longer possible to neglect interaction by surrounding atoms and the spectra give information on the local atomic structure as well. This technique is the so-called EXAFS spectroscopy (extended x-ray absorption fine structure) (Stern *et al* 1970, 1971).

The various XES and XAS spectral distributions are measured each one in its own x-ray transition energy scale. To obtain a representation of the occupied and unoccupied electronic bands (denoted as OB and UB respectively), which is helpful to analyse the electronic interactions, it is necessary to adjust the various partial DOS spectral curves on the same absolute energy scale, namely the binding energy scale. Such a purpose requires us to place the Fermi level energy (E_F) on each x-ray transition energy scale. This is made possible due to complementary measurements especially of inner levels binding energies from x-ray photoemission spectroscopy experiments (Belin and Traverse 1991).

2.3. Experimental procedure

Mg and Al K EXAFS and XAS (also denoted NEXAFS: near edge x-ray absorption fine structure) spectra probe unoccupied states of p character, since they correspond to transitions from the 1s level to continuum states. These spectra were measured at the Laboratoire pour l'Utilization du Rayonnement Electromagnétique (LURE, Orsay) with the Super ACO synchrotron radiation facility on the experimental station SA32. A double crystal monochromator was used, equipped with beryl or quartz $10\bar{1}0$ crystals for the Mg K and Al K spectra respectively. The x-ray beam was focused on the sample thanks to a toroidal mirror. The experiments were made at room temperature in the total electron yield mode (Gudat and Kunz 1972) by recording the drain current, I, from the samples whereas the incident beam intensity, I_0, was measured across a thin titanium film deposited by evaporation onto a polyester foil. As reference samples and for energy calibration purposes, pure Mg and Al sheets were also used. Note that the EXAFS Al spectra were recorded only up to 1780 eV, which is the Si K absorption threshold value, in order to avoid contribution from the silicon contained in the quartz monochromator.

Mg and Al K β-spectra probe 3p OB states owing to OB $\rightarrow$ 1s inner level transitions. They were analysed with bent crystal vacuum spectrometers using beryl or quartz $10\bar{1}0$ slabs for Mg and Al respectively. On the other hand, Mg and Al $L_{2,3}$ spectra, that scan 3s–d states due to OB $\rightarrow$ 2p transitions, were probed in a vacuum spectrometer fitted with a bent grating with 600 groves per mm. In all measurements, the samples, water cooled, were used as the targets of the x-ray tubes and irradiated with incoming electrons of about 2.5 keV. The emitted photons were detected by means of a gas flow Ar–CH_4 proportional counter or a photocathode plus a channeltron. The energy resolution was always of about 0.3 eV.

3. Results

3.1. EXAFS analysis

Standard procedures of normalization and background removal were used to determine the EXAFS oscillations χ versus the energy E of the photoelectron from I/I_0. The data were then converted to k space by applying $k^2/2m = E - E_0$, where E_0 is the threshold energy origin. The normalized EXAFS signal $k\chi_{(k)}$, shown in figures 1(a) and 1(b), looks different for Al and Mg edges. On the Al edge (figure 1(a)) the oscillations are very similar for both QP and β-phases. In contrast, differences are seen on the Mg edge (figure 1(b)) at about 3.6 Å^{-1}

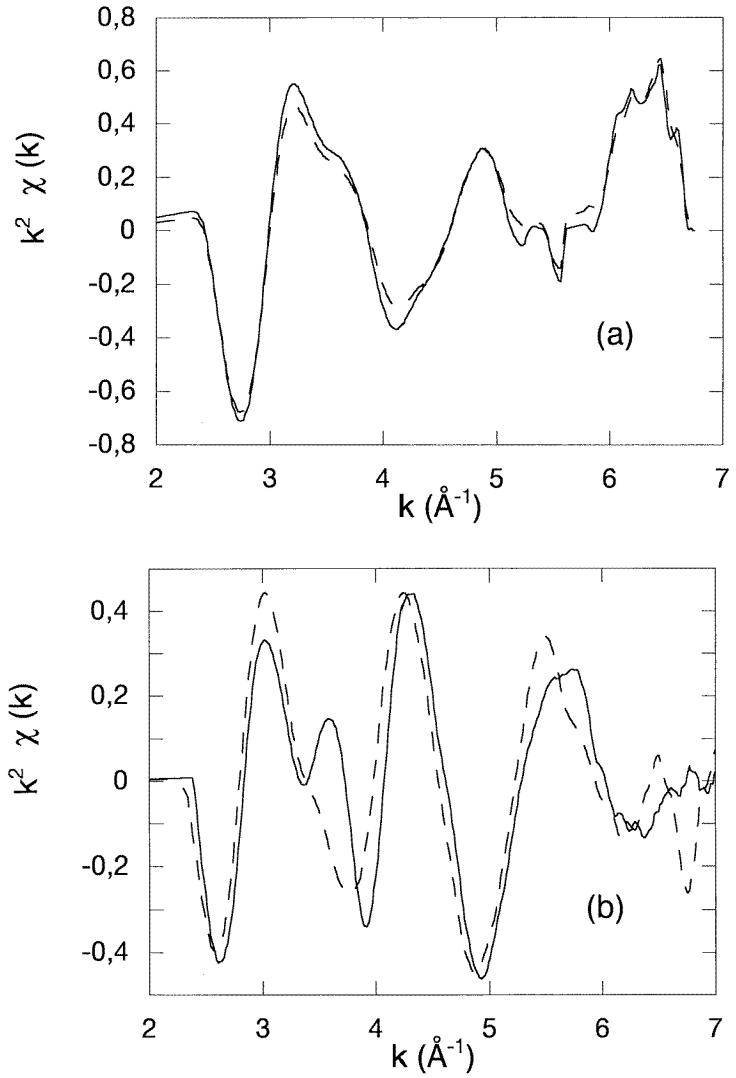

Figure 1. (a) EXAFS spectra of $k^2\chi(k)$ above the Al edge in β-Mg_2Al_3 (dashed line) and in quasiperiodic Mg–61 at.% Al alloy (solid line). (b) EXAFS spectra of $k^2\chi(k)$ above the Mg edge in β-Mg_2Al_3 (dashed line) and in quasiperiodic Mg–61% atom Al alloy (solid line).

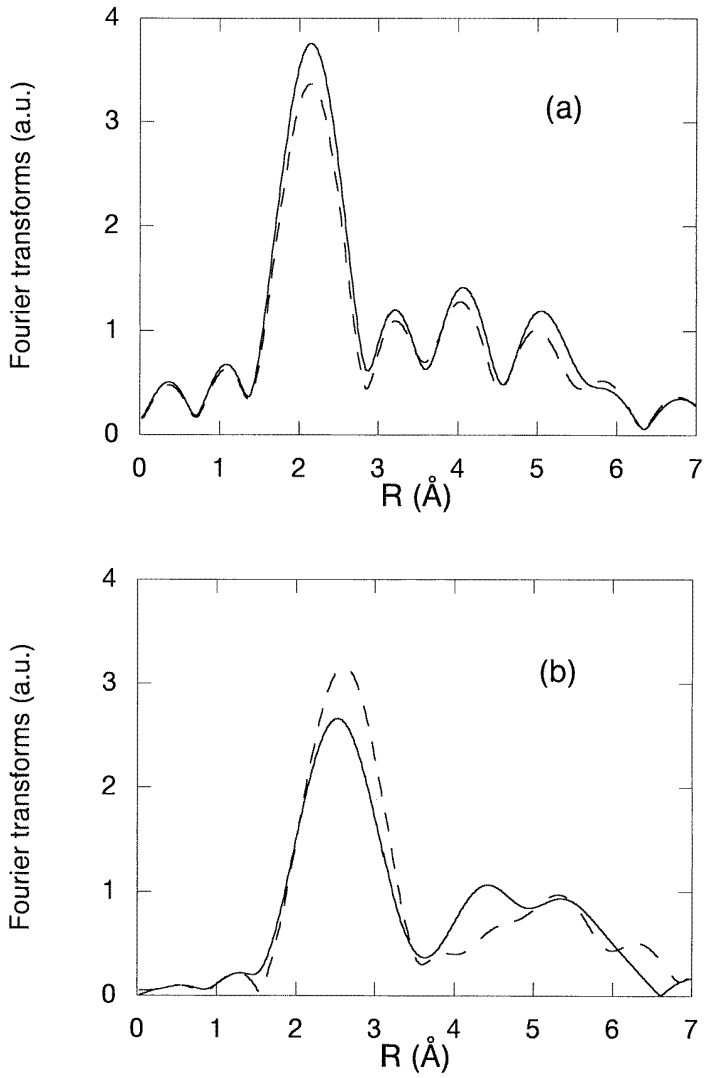

Figure 2. (a) Fourier transforms of $k^2\chi(k)$ above the Al edge in β-Mg_2Al_3 alloy (dashed line) and in quasiperiodic $Mg_{39}Al_{61}$ (solid line). (b) Fourier transforms of $k^2\chi(k)$ above the Mg edge in β-Mg_2Al_3 alloy (dashed line) and in quasiperiodic $Mg_{39}Al_{61}$ (solid line).

and 5.5 Å^{-1}. In addition, all Mg EXAFS spectra display strong destructive interference above 6 Å^{-1}.

The Fourier transforms (FT) to reciprocal space R of $k^2\chi(k)$ were then obtained using the same k-window from 2.5 Å^{-1} to 6.7 Å^{-1} for both Al and Mg K edges. Greater extent could have been taken on the Mg edge, but there is a poor signal to noise ratio for the β-phase. The FTs are qualitatively similar to the radial distributions of the atoms neighbouring the Al or Mg absorbing atom. However, the peaks are shifted to lower R distances because of the phase shifts experienced by the photoelectron while scattering from the potentials of the absorbing atom and nearest neighbours. They are shown in figures 2(a) and 2(b), which allow for a comparison between the crystalline and the QP state on the Al K edge and on the Mg K edge.

Above the Al K edge, the FTs exhibit a first neighbour peak centred at 2.1 Å (uncorrected for phase shift) and smaller peaks at further distances, which are very similar for both QP and β-phases. On the Mg K edge, the first neighbour peak is wider than for Al. Its maximum is shifted by 0.07 Å towards smaller R values for the QP phase with respect to the β-phase.

At further distances, the FTs look different in the 4–5 Å region. Thus, since the Al environments are identical, the Al–Mg pairs should be similar in the two alloys and consequently the differences observed in the 4–5 Å region in the FTs that correspond to the Mg K edge (figure 2(b)) must arise from Mg–Mg pairs.

To compare the co-ordination numbers, distances and disorder in the first co-ordination shell around Al and Mg atoms, the first neighbour peaks, between roughly 1.5 and 3.5 Å, were isolated and backtransformed to k-space. The inverse FTs were found to be nearly identical for the Al edge, but some differences remain on the Mg edge.

Thereafter, the Fourier-filtered spectra were fitted using the following formula (Stern *et al* 1975), which in single scattering theories describes the EXAFS oscillations for Gaussian distributions of neighbours around a central atom:

$$\chi(k) = -\sum_j \frac{N_j}{kR_j^2} B_j(k)\ \exp\left(-2\sigma_j^2 k^2 - \frac{2R_j}{\lambda}\right) \sin(2kR_j + 2\delta_j + \phi_j(k))$$

The sum is taken over shells with N_j atoms at distances R_j from the absorbing atom. σ_j is the mean square relative displacement of absorber and j backscatter atoms, so that the Debye–Waller factor $\exp(-2\sigma_j^2 k^2)$ is a measure of both static and dynamic disorder in shell j. $B_j(k)$ and $\phi_j(k)$ are the backscattering amplitude and the phase shift respectively, experienced by the photoelectron while scattering by the neighbours; δ_j is the phase shift of the central atom. $\lambda(k)$ is the electron mean free path and is taken to be of the form k/Γ (Lee and Pendry 1975), where Γ is a constant which was determined in the reference materials ($\Gamma = 0.7$ Å^{-2} for Al and 0.6 Å^{-2} for Mg). The amplitudes and phase shifts were taken from McKale *et al* (1988), who used a curved wave formalism in retaining the form of the traditional EXAFS equation. The fitting of the first neighbour peak in the FT was performed in both k- and R-spaces.

3.2. XES and XAS data

We will not give here details about fcc Al and pure Mg. Both elements which are well described in the free electron model have been extensively studied by means of SXES and SXAS. Let us recall that the Al 3p and Mg 3p distribution curves display an abrupt edge near to the Fermi level (E_F) followed by a parabolic-like decrease of intensity towards increasing binding energies and a broadening of the high binding energy wings due to Auger effects. Both Mg and Al 3s–d spectral curves exhibit a sharp narrow peak near E_F that is partly due to the presence of some states with a d-like character (Léonard 1978, Papaconstantopoulos 1986). Note that for both pure Mg and Al, the Fermi level is found exactly at the inflexion point of the edge of their 3p distribution curves. The alloys we study might not be free-electron-like. Hence, for a meaningful comparison between the elements pure or in the samples, we have normalized the 3p and 3s–d spectral curves to their maximum intensity. In such a procedure, if 100 is attributed to the maximum intensity of the 3p sub-bands for pure Al and Mg, the intensities of the inflexion points at E_F, denoted I_{E_F}, are equal to 50.

To perform the energy adjustments in order to obtain a picture of OB and UB of the QP phase and crystalline β-Mg_2Al_3, we have measured the binding energies of their Mg and Al 2p levels. As compared to the pure metals, we found that they are shifted towards increasing binding energies by 0.3 and 0.2 ± 0.1 eV for Mg and Al respectively in the crystalline alloy against 0.5 and 0.3 ± 0.1 eV respectively in the QP phase.

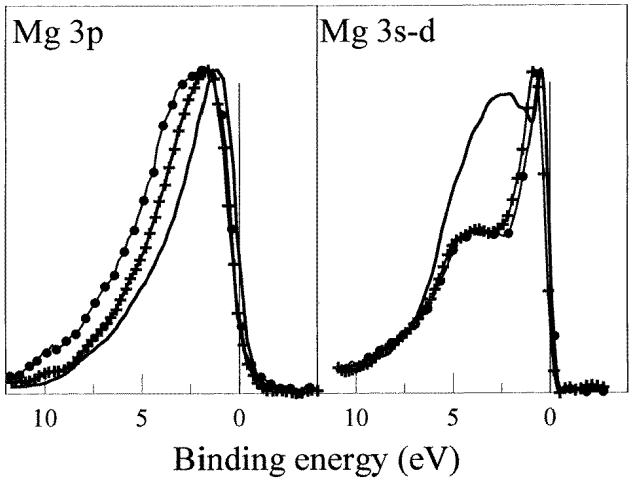

Figure 3. Mg 3p (left panel) and 3s–d (right panel) states curves for pure Mg (solid), QP phase (line with crosses) and crystalline β-Mg_2Al_3 (line with full circles). The curves are normalized in the intensity scale to their maxima.

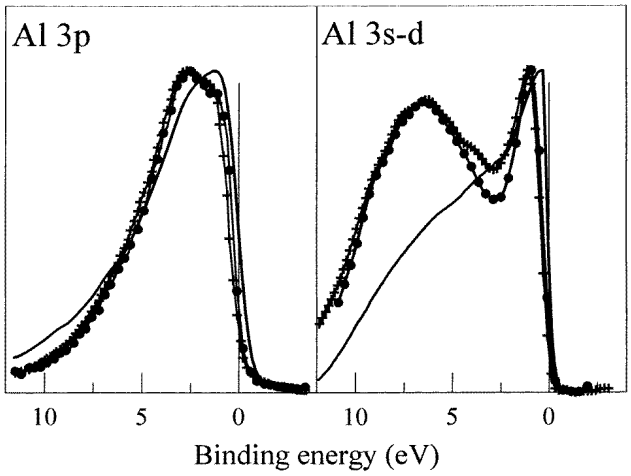

Figure 4. Al 3p (left panel) and 3s–d (right panel) states curves for pure Al (solid line), QP phase (line with crosses) and crystalline β-Mg_2Al_3 (line with full circles). The curves are normalized in the intensity scale to their maxima.

Figures 3 and 4 for Mg and Al respectively show that the shapes of the OB 3s–d spectral curves significantly differ in the alloys as compared to the pure metals whereas this is not the case for the 3p ones. However, it is worth noting that the Mg 3p curves in alloys are broader than in the metal: their full widths at half maximum intensity (FWHMs) are 5.0 and 4.0 ± 0.1 eV respectively in β-Mg_2Al_3 and the QP alloy against 3.4 ± 0.1 eV in pure Mg. Their maxima in β-Mg_2Al_3 and the QP phase are at 1.6 ± 0.1 eV to compare with 1.1 ± 0.1 eV in pure Mg. For Al 3p, the FWHMs are 5.1 ± 0.1 eV in the two crystalline and QP alloys and 5.3 ± 0.1 eV in fcc Al. The Al 3p maxima for β-Mg_2Al_3 and QP phases are also at the same

energy but shifted by about 1.5 eV with respect to pure Al. Within the experimental accuracy, the Mg or Al 3p edges are parallel (see figures 3 and 4) but their inflexion points are distant from E_F by 0.4 ± 0.1 eV and $0.5_5 \pm 0.1$ eV for Mg 3p in β-Mg_2Al_3 and QP phase whereas this distance is $0.3_5 \pm 0.1$ eV and $0.5_5 \pm 0.1$ eV for Al 3p in β-Mg_2Al_3 and the QP phase. As a consequence the Mg 3p and Al 3p intensities I_{E_F}, are less than 50%, namely about 26% in β-Mg_2Al_3 against about 17 % in the QP phase. The shapes of the 3s–d spectral curves are also very similar for β-Mg_2Al_3 and the QP phase but dramatically depart from the pure metals. For both Mg and Al, 3s–d curves of the alloys exhibit a prominent peak which is much larger than the narrow peak observed in the pure metals. The maxima of the peaks are at $+0.8 \pm 0.1$ eV for Mg and $+0.6 \pm 0.1$ eV for Al. For both Mg and Al in the alloys, this peak is followed by a marked minimum around 2 eV, i.e. in the energy range of the Mg and Al 3p maxima. The Mg 3s–d curves for the alloys display a 2 eV wide plateau below 3 eV from E_F that is followed by a monotonic decrease of intensity. The Mg 3s–d curves are much narrower than the Al 3s–d ones. In this latter case, there is an important broad maximum within 5 to 9 eV from E_F. The minimum between the peak near E_F and this broad feature is more contrasted for β-Mg_2Al_3 than for the QP phase. Note that our results for β-Mg_2Al_3 agree fairly well with previous data from Neddermeyer (1973).

The curves for the unoccupied Al p states in pure fcc Al, β-Mg_2Al_3 and QP alloy, normalized to their maximum intensities, plotted in the x-ray transition energy scale, are displayed in figure 5. The inset of this figure shows the same curves, again for QP alloy as well as for Al in Al_2O_3. This points out that to get rid of any possible oxide contamination one can carefully consider the unoccupied states beyond 4 to 5 eV from E_F. This is also true for Mg, which is even much more oxidizable than Al. Figure 6 displays the unoccupied Mg p state distributions in pure MgO and in Mg partly oxidized. Thus, in the following, although the Al spectra show no severe contribution from oxide, since this is not the case for Mg we will only pay attention to the unoccupied distributions within 4 eV from E_F.

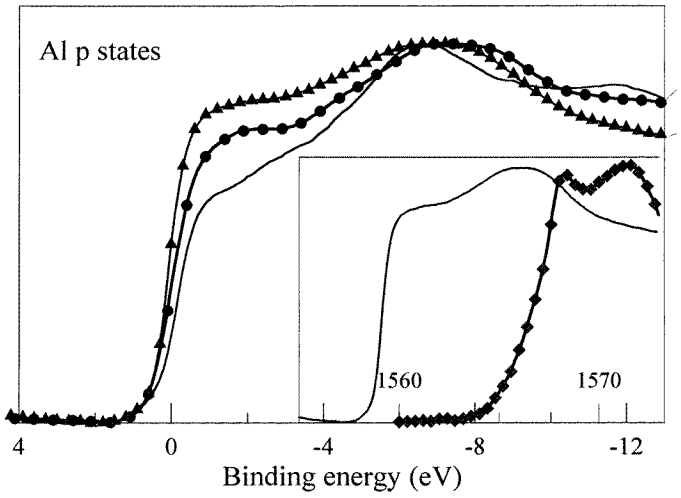

Figure 5. Al p distribution curves normalized to the maximum intensity for fcc Al (thin line), β-Mg_2Al_3 (line with full circles) and the QP phase (line with full triangles). In the insert, Al p distribution curves for the QP phase (thin line) and for Al_2O_3 (thick line with diamonds) as normalized to their maximum intensities are given in the x-ray transition energy scale.

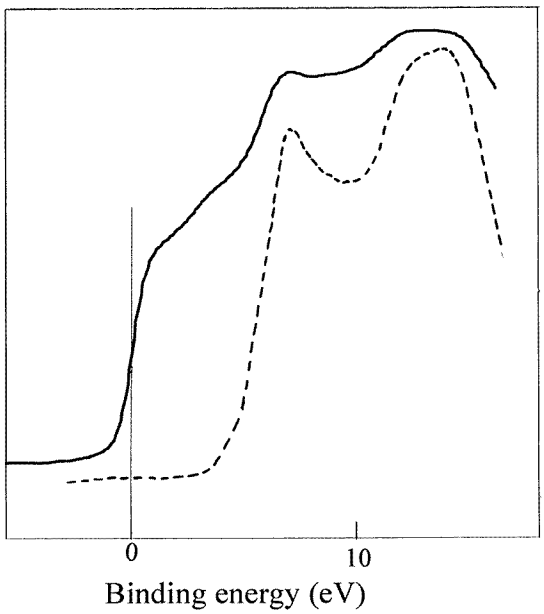

Figure 6. Mg p distribution curves in MgO (dashed line) and in Mg slightly oxidized (solid line) normalized in the intensity scale to their maxima. For clarity, the curves are shifted in the intensity scale.

4. Discussion

4.1. First neighbour distributions

The EXAFS measurements and analysis have pointed out that the local order around Al atoms in the QP state and in the crystal should be the same and that differences are seen as far as Mg–Mg environments are concerned.

To go a step further in the analysis and discussion of the EXAFS data, some knowledge of the β-phase model is needed. This crystalline structure was described by Samson (1965) with some uncertainty that arises from the fact that it is difficult to determine by x-ray diffraction techniques the exact distributions of the Mg and Al atoms over the occupied positions. There are approximately 1168 atoms in the unit cell, which are distributed over 23 different crystallographic positions with occupancies less than 100% for half of the sites. The unit cube contains 672 icosahedra, 252 Friauf polyhedra, which are truncated tetrahedra, and 244 miscellaneous more or less irregular polyhedra. All atoms except 24 among the 720 Al atoms in the unit structure are surrounded by 12 crystallographic sites. However, the occupancy of these sites can be less than 1, which leads to a mean co-ordination number less than 12 atoms around Al atoms. It is the same for Mg atoms surrounded by Friauf polyhedra of ligancy 16 and other types of polyhedron of ligancy 10 to 16, which gives a mean co-ordination number of about 13.7 atoms around Mg atoms.

Using the crystallographic model of Samson, the distributions of the first atomic distances were computed for Al–Al, Al–Mg and Mg–Mg pairs. The Al–Al distances range from 2.562 to 3.568 Å, with on average 4.8 Al at 2.74 Å from an Al atom. The Al–Mg distances range from 2.509 to 3.754 Å, with on average 5.8 Mg at 3.18 Å from an Al atom or 8.7 Al around one Mg atom. The Mg–Mg distances are grouped within 2.799 to 3.868 Å, with on average

5 Mg at 3.28 Å from an Mg atom. Therefore, there are 10.6 first neighbour atoms around one Al atom and 13.7 around one Mg atom. The frequencies of these first distances, obtained by coupling together similar distances which differ by less than 0.03 Å, are shown in figure 7. The distribution is narrow for the Al–Al pairs but very broad for the Mg–Mg pairs, with a first maximum at 3.08 Å and a second one at 3.32 Å, yielding roughly to three domains with, on average, 1.2 Mg atoms at 3.01 Å, 2.9 Mg at 3.30 Å and 1 Mg at 3.55 Å. The average co-ordination numbers and distances are shown in table 1.

Table 1. First neighbour shells of Al and Mg atoms in β-Mg_2Al_3 and QP MgAl. $\Delta N = \pm 1$ atom, $\Delta R = \pm 0.05$ Å, $\Delta\sigma = \pm 0.02$ Å. The figures in parentheses are the parameters of the fit taking account of a second Mg–Mg distance.

	β-Mg_2Al_3					QP MgAl		
	X-ray diffraction Samson's model		EXAFS			EXAFS		
Central atom	$\bar{N}$	$\bar{R}$ (Å)	N	R (Å)	σ (Å)	N	R (Å)	σ (Å)
Al	4.8 Al	2.74	4.8 Al	2.70	0.16	4.8 Al	2.75	0.16
	5.8 Mg	3.18	5.8 Mg	3.15	0.21	5.8 Mg	3.19	0.21
Mg	8.7 Al	3.18	8.7 (7) Al	3.18 (3.13)	0.21 (0.24)	8.5 (7) Al	3.14 (3.19)	0.22 (0.24)
	1.2 Mg	3.01	1.5 (1.7) Mg	3.03 (2.97)	0.10 (0.11)	1.5 (2) Mg	2.99 (2.95)	0.12 (0.13)
	2.9 Mg	3.30	0 (3) Mg	(3.23)	(0.15)	0 (2.5) Mg	(3.16)	(0.15)
	1 Mg	3.55						

Starting with these data, the filtered EXAFS spectra for β-Mg_2Al_3 were reconstructed, on the Al edge, with co-ordination numbers N and distances R which differ respectively from the average crystallographic values, $\bar{N}$ and $\bar{R}$, by about 0.3 atom and 0.03 Å (table 1). It must also be kept in mind that there is some uncertainty in the crystallographic structure. On the Mg edge, a first model (table 1) involving Mg–Al pairs and one Mg–Mg distance, at 3.03 Å, was found to reconstruct the experimental EXAFS spectrum of the β-phase. The experimental modulus and imaginary part of the Fourier transforms for the first shell of neighbours are compared in figure 8 (uncorrected for phase shift) with their simulation. However, these experimental spectra on the Mg edge could as well be fitted using in addition a second Mg–Mg distance at 3.23 Å, which corresponds to the main peak in the radial distribution of Mg–Mg distances (figure 7), according to Samson's model. Of course, it was necessary to change the other parameters of the fit, given in parentheses in table 1, which differ only slightly from the first set of parameters and from the average crystallographic values, confirming thus the Samson model.

Then the filtered EXAFS spectra for the QP phase were simulated using N_j, R_j- and σ_j values which are very close to those obtained for the β-phase. As a matter of fact, the figures obtained for N_j, R_j and σ_j-parameters were found the same for both phases within the experimental errors, $\Delta N_j = \pm 1$ atom, $\Delta R_j = \pm 0.05$ Å, $\Delta\sigma_j = \pm 0.02$ Å (table 1). The great disorder parameter values which were obtained well reflect the very broad distributions of distances.

Finally, the first neighbourhood around Al and Mg atoms is found to be identical in both QP and crystalline phases, as suspected from the comparison between FTs. The most obvious difference lies in the medium range order around Mg atoms, at distances of 4–5 Å.

Our EXAFS measurements have confirmed the local structure proposed for β-Mg_2Al_3 by Samson (1965). Actually, because of the complexity of this crystalline alloy, no check of the model was done after the earlier x-ray work by Samson (1965). Thus, since the first neighbourhood in the QP phase agrees with the Samson model for β-Mg_2Al_3, we can further

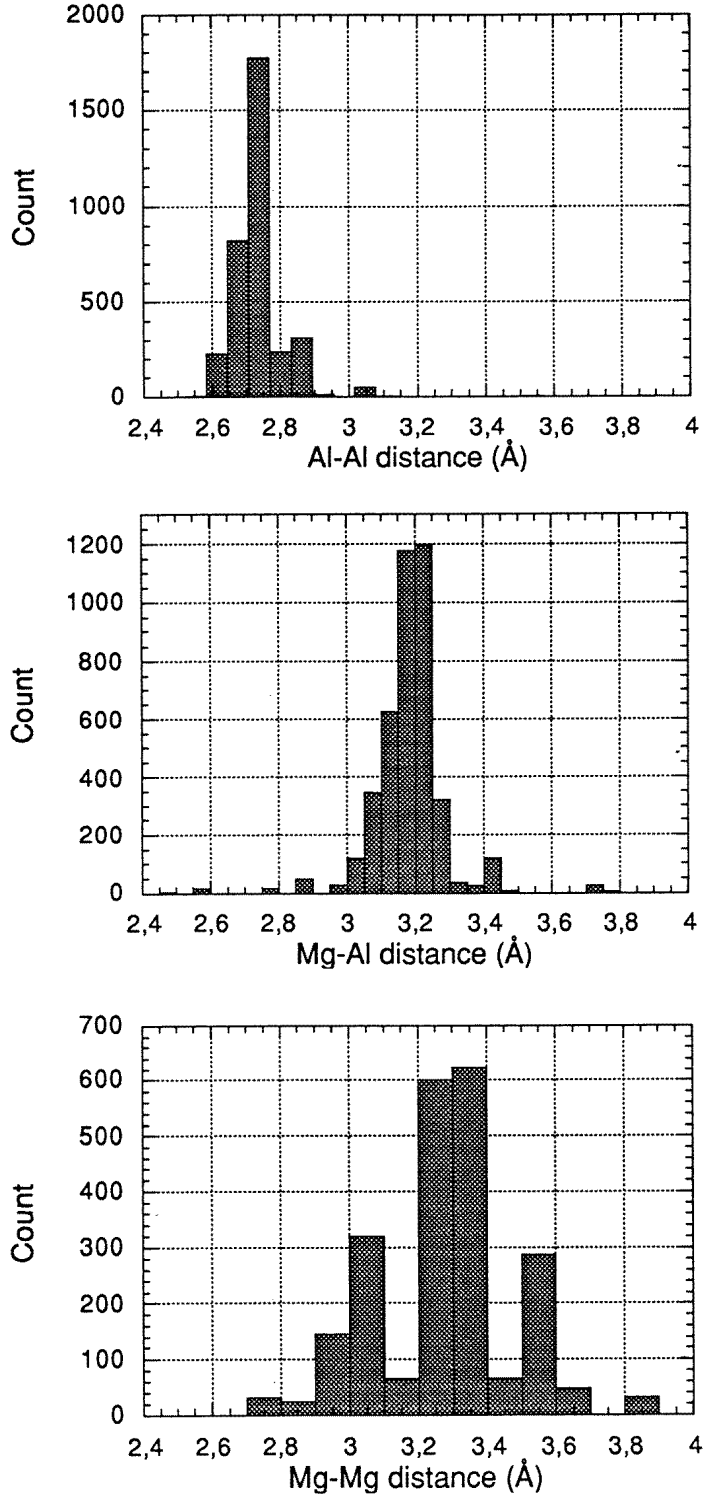

Figure 7. Frequencies of the first Al–Al, Al–Mg and Mg–Mg distances in β-Mg_2Al_3.

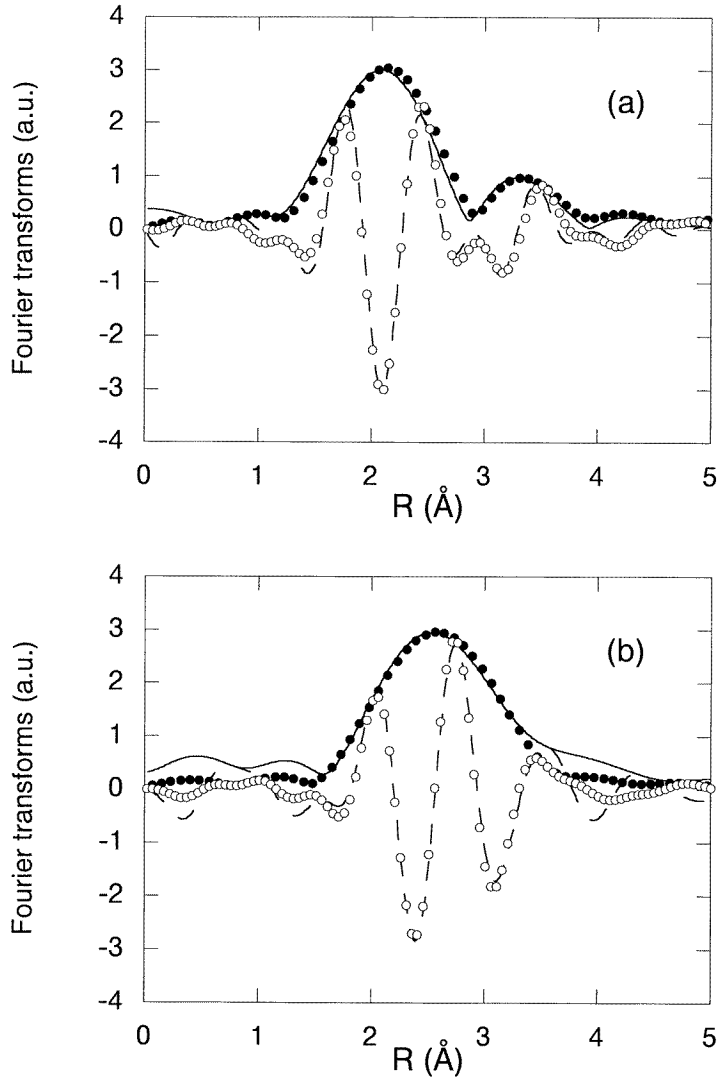

Figure 8. (a) Modulus (solid circles) and imaginary part (open circles) of the Fourier transform for the first shell of neighbours at the Al edge in β-Mg_2Al_3. Solid and broken lines show their simulation, respectively. (b) Same as in (a) but for the Mg edge in β-Mg_2Al_3. All intensities are in arbitrary units.

use this model to interpret the differences concerning the medium range order. Therefore, let us recall other details of the β-Mg_2Al_3 structure model as proposed by Samson (1965), which is based on a packing of clusters.

The basic cluster is a ring formed by five face-sharing Friauf polyhedra; the Friauf polyhedron is occupied by an Mg atom in its centre. The next entity is built by a large octahedron decorated by fivefold rings. This cluster which contains, besides the six rings of Friauf polyhedra, icosahedral clusters, constitutes a 234-atom aggregate. The large clusters (Td) when meshed according to a cubic symmetry are related to one another to a diamond glide. It is possible to build a continuous 3 dimension network with the Td clusters. From

that basis, Samson (1965) has drawn an idealized model and a disordered model: only the disordered model fits with the x-ray data. This disordered model can be seen in terms of modification of the linkage between the Td cluster description or equivalently in terms of modification of some sites in the fivefold rings of Friauf polyhedra. In the idealized model, the linkage between the Td clusters is made by 21-atom clusters centred on Mg clusters. There are eight linkage clusters per cell. In β-Mg_2Al_3, to fit with the experimental x-ray data, it was necessary to modify these linkage clusters: they became 15-atom clusters still centred on an Mg atom. In terms of the fivefold Friauf polyhedron rings, the modification consisted in partial occupation and position changes for two neighbouring Friauf polyhedra. The shell of the Al atoms around the Mg atoms at the centre of a Friauf polyhedron has a radius within 3–3.3 Å and the distance separating the Mg atoms concerned by the modification is about 4 to 5 Å, which also corresponds to the medium range order where differences between β- and QP phases are observed by EXAFS around Mg atoms. A modification of the Mg atoms at the centre of the Friauf polyhedra linking the Td clusters produces no deviation in the Al–Al distribution. Besides, since these linkage clusters are quite few (only eight per cell in the β-phase structure), the Al–Mg distance distribution should not be strongly changed. On the other hand, modifying the Mg atoms at the centre of the linkage clusters necessarily affects the Mg–Mg distance in the 4 to 5 Å range.

Consequently, because of the similarities between β-Mg_2Al_3 and the QP phase, we suggest the large cluster proposed by Samson (1965) can be considered as a starting basis for modelling the QP phase and thus we interpret the change observed in the medium range order in the QP state as a modification of the linkage between clusters, leading from a periodic structure to a quasiperiodic one.

4.2. Electronic structure

Let us recall that the main features of partial local densities of states arise mostly from the local environment of the probed atom; however, whereas localized states are more concerned by first neighbours, the extended states are also sensitive to medium range order. Figures 9 and 10 show all the sub-bands which we have investigated as adjusted to the binding energy scale. In the OB, the sub-bands are normalized to their maxima and the UB curves for the Mg and Al p states are adjusted to the same intensity at E_F as the corresponding 3p distributions. We will come back later to this point.

We have already mentioned that in pure Mg and Al states are completely sp hybridized over the whole extent of the OB with some d contribution in the close vicinity of E_F. In the alloys, from the Fermi level to increasing binding energies, over 2 eV from E_F, one finds large peaks which, by analogy to pure Al or Mg, should correspond to states with some d-like character; indeed, these peaks are too far from E_F to be ascribed to the infra-red catastrophe which is observed in free-electron-like systems (Nozières and de Dominicis 1969). Then the Mg and Al 3p states overlap the minimum of the 3s–d distribution over about 1 eV, beyond they are hybridized to the s states in the energy range 2–4 eV, finally Al s states, almost pure, are present beyond 4 eV from E_F. It is to be noticed that, in the QP phase, the peaks corresponding to 3d–s states are broader than in β-Mg_2Al_3. This can be interpreted as giving an indication that there are states with d-like character over a larger energy range in the QP phase than in its crystalline counterpart. On the other hand, the fact that the Mg 3p states extent is narrower in the QP phase than in β-Mg_2Al_3 brings an indication that the corresponding states are energetically more confined in the QP than in the crystalline alloy. Thus altogether, states in the QP phase are somewhat more localized-like than in crystalline β-Mg_2Al_3. We have reported in the above paragraph that the Mg and Al 3p edges are at a larger distance

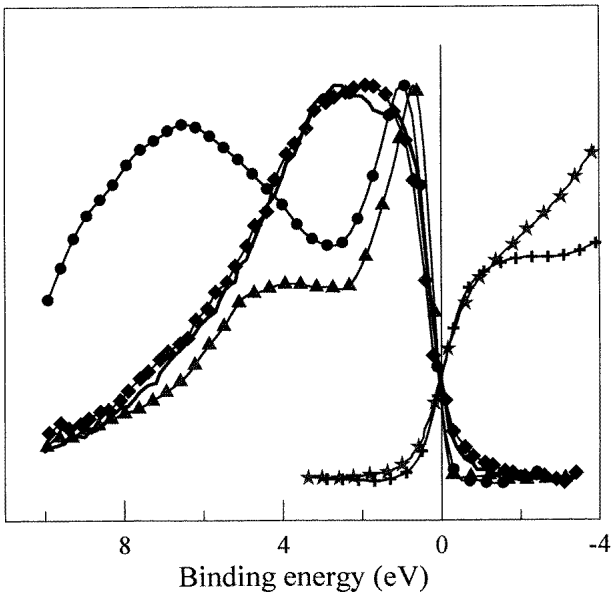

Figure 9. OB (left side) and UB p-like states (right side) in β-Mg_2Al_3: Mg 3p = line with squares, Mg 3s–d = line with triangles, Al 3p = solid line, Al 3s–d = line with full circles, Mg p = line with stars, Al p = line with crosses. The OB distribution curves are normalized to their maxima. The Al and Mg p-like distributions are normalized to the same intensity at the Fermi energy as the corresponding 3p curves (see text).

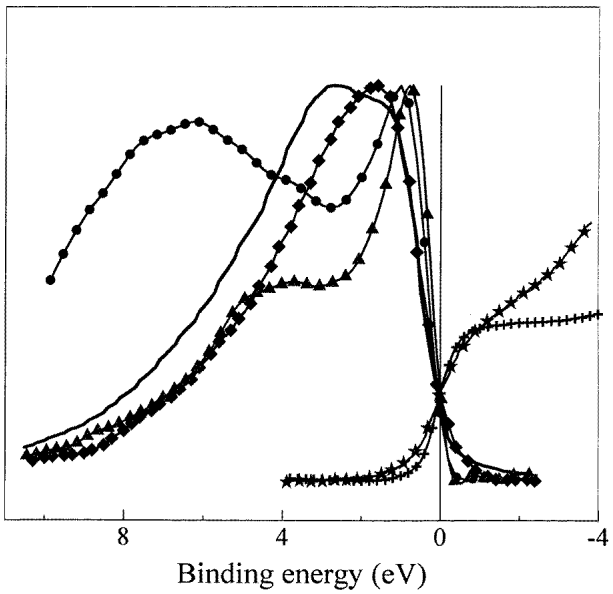

Figure 10. OB (left side) and UB p-like states (right side) in QP $Mg_{39}Al_{61}$ alloy: Mg 3p = line with diamonds, Mg 3s–d = line with triangles, Al 3p = solid line, Al 3s–d = line with full circles, Mg p = line with stars, Al p = line with crosses. The OB distribution curves are normalized to their maxima. The Al and Mg p-like distributions are normalized to the same intensity at the Fermi energy as the corresponding 3p curves (see text).

from E_F than in β-Mg_2Al_3. Let us recall here that Terakura (1977) described by theoretical means the interaction between a relatively narrow d band and a broad sp band in terms of a Fano-like effect irrespective of the relative concentrations of the d and sp bands. The result of such an interaction is to induce an asymmetric deformation of the sp band leading to the creation of a hybridization gap which splits the sp states into two parts located on each side of the d band peak. In our alloys both extended and localized states are present. By analogy to the 'Terakura-Fano' model, we assume a similar kind of interaction between the d-like states close to E_F and the more extended s–p-like states whose result is to repel these latter states from E_F. Consequently the intensities at E_F of the Mg 3p and Al 3p spectra are no longer 50% as in pure Mg or Al. They are $26 \pm 0.2\%$ in β-Mg_2Al_3 against $17 \pm 0.2\%$ in the QP phase where there are more d states near E_F than in the crystalline alloy. So, a depletion in the electronic distributions forms at E_F, which we denote as a 'pseudo-gap'. This is larger for the QP phase than for the crystalline counterpart. The formation of this pseudo-gap due to an electronic Hume–Rothery-like mechanism arising from the contact between the Fermi sphere and the planes of the Brillouin zone might not be essential here; indeed, in the Frank–Kasper Mg–Al system, the structure can be stabilized by a size effect between the large Mg and small Al atoms, since the ratio between Mg and Al atomic volumes is 0.63. A ratio value of 0.65 induces the maximum compacity for the structure.

We have normalized in figures 9 and 10 the Mg and Al occupied 3p and unoccupied p curves to the same intensity at E_F of β-Mg_2Al_3 and the QP phase respectively which assumes that the distribution of a given spectral character is a continuous function of the energy. Accordingly, the intensities at E_F of OB or UB with the same spectral character should be identical. The same adjustment is made for pure Mg and Al in figures 11(a) and 11(b) respectively. We observe a relative flattening of both Al and Mg p bands in the alloys with respect to the pure metals. Over about 2 eV from E_F, the Mg and Al p sub-bands overlap (figures 9 and 10) and then at further energy distance, the Mg sub-bands are more intense. Altogether this points out a complete mixing of the conduction bands in the alloys. In addition, we observe that the conduction sub-bands are less intense in the QP phase than in the crystalline alloy, that points out a larger pseudo-gap between the occupied 3p and unoccupied p bands for the QP phase than its crystalline counterpart.

These conclusions are reminiscent of those derived from the same methodology for Al (or Mg) based quasicrystals and related crystalline alloys. Let us recall that in the occupied states, in the close vicinity of E_F interaction exists between Al 3p–s,d states and transition metal states of d character, the result of which is to open a pseudo-gap in particular in the Al distribution of p character whereas the occupied Al s-like states are pushed far away from E_F. The pseudo-gap has been found wider and deeper in quasicrystals than in approximants. Furthermore, adjustment of the Al p unoccupied states curves to the occupied Al 3p ones, as described above, shows a progressive flattening of the Al p sub-bands when going from pure fcc Al to approximants and quasicrystals emphasizing thus the progressive loss of metallic character from the free electron metal to the highly resistive quasicrystalline alloys (Belin *et al* 1992, Belin-Ferré and Dubois 1996, Belin-Ferré *et al* 1997). Our results for quasicrystals are in good agreement with the model of Janot and de Boissieu (1994), from which the stability of the quasicrystals is assigned to the localization of electrons in a succession of inflated spherical quantum wells attached to hierarchical generations of clusters of atoms, the inflation ratio being related to the golden mean τ. In this model, most of the electronic states form a semi-bonded occupied band that sharply decreases at E_F detrimentally to the extended conduction band which is of very flat intensity. Both bands are split at the Fermi level by an asymmetric valley. Note that in the approximants clusters also are present but periodically arranged in the network (Quiquandon *et al* 1995, Quivy *et al* 1996).

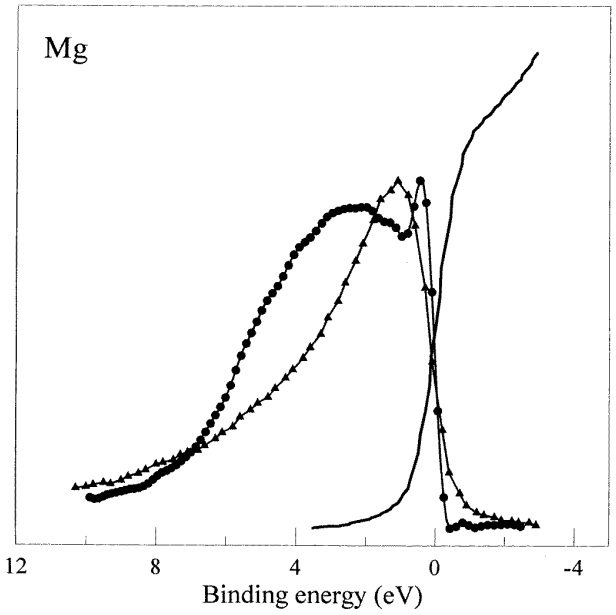

(a)

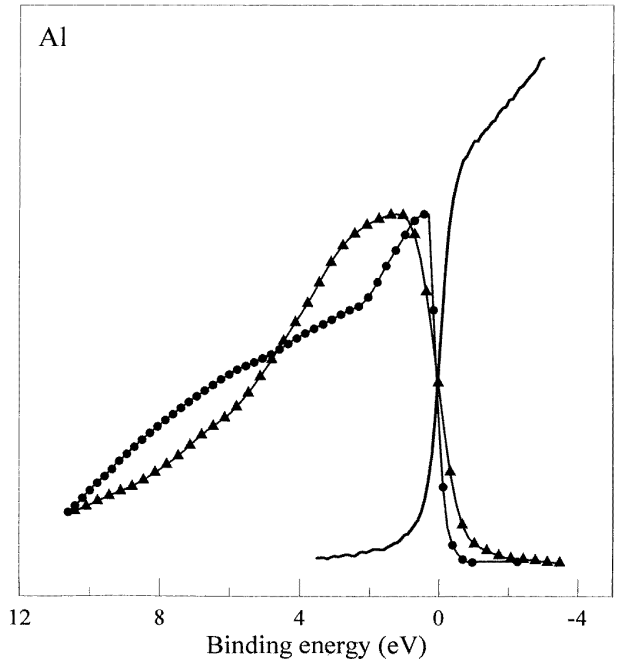

(b)

Figure 11. (a) OB (left side) and UB p-like states (right side) in pure Mg: Mg 3p = line with triangles, Mg 3s–d = line with full circles, Mg p = solid line. The p-like distributions are normalized to the same intensity at the Fermi energy (see text). (b) OB (left side) and UB p-like states (right side) in pure Al: Al 3p = line with triangles, Al 3s–d = line with full circles, Al p = solid line. The p-like distributions are normalized to the same intensity at the Fermi energy (see text).

In the present work, the β-Mg_2Al_3 is also built from clusters, in the QP phase analogous clusters inflate quasiperiodically according to a ratio related to $(2 + \sqrt{3})$. Thus, our results suggest that the enhancement of the pseudogap in quasiperiodic structures, as we observed in quasicrystalline alloys, results from the occurrence of the hierarchy of the unit cluster entities.

5. Conclusion

EXAFS experiments performed in QP and β-Mg_2Al_3 alloys show that: (i) the first neighbourhoods around Al and Mg atoms are identical in both phases, (ii) some difference exists in the Mg environment but in a medium range order, at about 4–5 Å from Mg atoms. An explanation is that both the crystalline and quasiperiodic phases are built with the same structural units but linked in a different way. This interpretation follows general observations made for icosahedral cluster structures (Shoemaker and Shoemaker 1988) and confirmed by EXAFS (Sadoc *et al* 1993) for icosahedral $Al_{63}Cu_{24.5}Fe_{12.5}$ and for the rhombohedral approximant $Al_{62.8}Cu_{26}Fe_{11.2}$, a 3/2 approximant of the icosahedral phase, where the same first environments were found.

The differences shown in the Mg neighbourhood, though small, might be highly relevant because of the specific part played by the Mg atoms in the structure. It is worth noting that, in Samson's model, the position and occupancy of some Mg sites in the idealized model have to be modified to obtain a structure consistent with the β-phase crystal. In other words, the structural disorder essentially affects the linkage clusters which are centred on part of the Mg atoms. On the other hand, Mg atoms frequently occupy the centre of Friauf polyhedra and thus inherit the packing ability and frustration of the tetrahedron. As the Samson model appears essentially correct for the β-phase structure, the large Td clusters should be kept in the elaboration of a structural model for the QP state. The problem remains then to propose a manner to link these large clusters which introduces quasiperiodicity and inflation symmetry.

The investigation of the electronic structure also points out significant modifications around Mg atoms, namely larger shift of inner levels and larger shift of the 3p sub-band edge, as compared to Al. This confirms the conclusions of the study of the atomic structure and points out that not only local order but also medium order changes are perceptible in the electronic distributions.

On the other hand, similarities have been found between previous results for quasicrystals and approximants and the present Mg–Al system. In all these alloys, a significant pseudo-gap is seen at the Fermi level in the electronic distributions which is more marked in the quasicrystalline or quasiperiodic structures than in the crystalline counterparts. From the present data and our previous results we propose that the enhancement of the pseudo-gap in the non-periodic structures as compared to the related crystals is due to the occurrence of the inflation mechanism.

Acknowledgments

We thank Z Dankházi for help during measurements and P Ochin for assistance in sample preparation. Allocation of beam time by the Laboratoire de l'Accélérateur Linéaire (LURE) is gratefully acknowledged. This work has been supported in part by the Austrian Ministry of Research, East–West co-operation programme under the title 'Soft x-ray spectroscopy of metallic systems'. VF and EB-F express their gratitude to Professor H Kirchmayr for his hospitality at the Technical University of Vienna (Austria). EB-F dedicates this paper to the memory of her friend Dr Christiane Sénémaud.

References

Agarwal B K 1979 *X-ray Spectroscopy. An Introduction* (Berlin: Springer)

Belin E, Dankházi Z, Sadoc A, Calvayrac Y, Klein T and Dubois J M 1992 *J. Phys.: Condens. Matter* **4** 4459

Belin E and Traverse A 1991 *J. Phys.: Condens. Matter* **3** 2157

Belin-Ferré E and Dubois J M 1996 *J. Phys.: Condens. Matter* **8** L717 and references therein

Belin-Ferré E, Fournée V, Donnadieu P, Dankházi Z and Harmelin M 1998 *Quasicrystals* ed S Takeuchi and T Fujiwara (Singapore: World Scientific) p 619

Belin-Ferré E, Fournée V and Dubois J M 1997 *New Horizons in Quasicrystals: Research and Applications* ed A I Goldman, D J Sordelet, P A Thiel and J M Dubois (Singapore: World Scientific) p 9

Bonnelle C 1987 *Annual Report C, The Royal Society of Chemistry* pp 201–72

Donnadieu P, Su H L, Proult A, Harmelin M, Effenberg G and Aldinger F 1996 *J. Physique* **6** 1153

Fournée V, Belin-Ferré E, Sadoc, Donnadieu P and Ochin P 1998 *Proc. Aperiodic'97* ed J L Verger-Gaugry *et al* (Singapore: World Scientific) at press

Gudat W and Kunz C 1972 *Phys. Rev. Lett.* **72** 1674

Janot C and de Boissieu M 1994 *Phys. Rev. Lett.* **29** 169

Lee P A and Pendry J B 1975 *Phys. Rev.* B **11** 2795

Léonard P 1978 *J. Phys. F: Met. Phys.* **8** 467

McKale A G, Veal B W, Paulikas A P, Chan S K and Knapp G S 1988 *J. Amer. Chem. Soc.* **110** 3763

Neddermeyer H 1973 *Band Structure Spectroscopy of Metals and Alloys* ed D J Fabian and L M Watson (London: Academic) p 153

Nozières P and de Dominicis C T 1969 *Phys. Rev.* **178** 6105

Papaconstantopoulos D A 1986 *Handbook of the Band Structures of Elemental Solids* (New York: Plenum)

Quiquandon M, Quivy A, Devaud, Faudot F, Lefèbvre S, Bessière M and Calvayrac Y 1996 *J. Phys.: Condens. Matter* **8** 2487

Quiquandon M, Quivy A, Faudot F, Sâadi N, Calvayrac Y, Lefèbvre S and Bessière M 1995 *Quasicrystals* ed C Janot and R Mosseri (Singapore: World Scientific) p 152

Quivy A, Quiquandon M, Calvayrac Y, Faudot F, Gratias D, Berger C, Brand R A, Simonet V and Hippert F 1996 *J. Phys.: Condens. Matter* **8** 4223

Sadoc A, Berger C and Calvayrac Y 1993 *Phil. Mag.* B **68** 475

Sadoc A, Donnadieu P and Flank A M 1998 *Proc. Aperiodic'97* ed J L Verger-Gaugry *et al* (Singapore: World Scientific) at press

Samson S 1965 *Acta Crystallogr.* **19** 401

Shoemaker D P and Shoemaker C B 1988 *Introduction to Quasicrystals* ed M Jaric (London: Academic) pp 3–57

Stern E A, Sayers D E and Lytle F W 1970 *Adv. X-ray Anal.* **13** 248

——1971 *Phys. Rev. Lett.* **27** 1204.

——1975 *Phys. Rev.* B **11** 4836

Terakura K 1977 *J. Phys. F: Met. Phys.* **7** 1773

Yamamoto A 1982 *Acta Crystallogr.* B **38** 1451